

Statistics of light in Raman and Brillouin nonlinear couplers

J. Peřina, Jr. and J. Peřina

Joint Laboratory of Optics, Palacký University and
Institute of Physics of Academy of Sciences of the Czech Republic
and

Laboratory of Quantum Optics
Department of Optics, Palacký University
17. listopadu 50, 772 07 Olomouc, Czech Republic

Abstract

Statistical properties of optical fields in nonlinear couplers composed of two waveguides in which Raman or Brillouin processes (with classical pumping) are in operation and which are mutually connected through the mutual Stokes and/or anti-Stokes linear interactions are investigated in the framework of a generalized superposition of coherent fields and quantum noise. Heisenberg equations describing the couplers are solved both analytically under special conditions and numerically in general cases. Regimes for nonclassical properties of optical fields, such as sub-Poissonian photon number statistics, negative reduced moments of integrated intensity, and squeezing of quadrature fluctuations are discussed in cases of single and compound fields. General results are compared with those from the short-length approximation.

1 Introduction

Recently increasing attention has been devoted to the study of nonlinear couplers composed of two or more waveguides with mutually connected modes by means of evanescent waves [1, 2, 3]. Also quantum statistical properties of such devices have been studied [4, 2]. Especially, couplers composed of linear and nonlinear waveguides have been examined for both directional [5, 6] and contradirectional [6, 7] propagation of light beams. Also couplers composed of two nonlinear waveguides have been investigated [8]. Various nonlinear optical processes were assumed to operate in nonlinear waveguides, such as second harmonic generation [8] (and references therein), frequency downconversion [9, 10, 11, 12] and Kerr effect [13, 14, 15].

We examine quantum statistical properties of couplers composed of two waveguides in which Raman or Brillouin processes are active and in which modes (Stokes and anti-Stokes) mutually linearly interact through evanescent waves. We suppose classical strong laser pumping of the nonlinear processes in both the waveguides. Then we can apply the method of the generalized superposition of coherent fields and quantum noise to study spatial dependence of statistical quantities, such as photon number distribution, reduced moments of integrated intensity, quadrature variances and principal squeeze variance for both single and compound modes. Special attention is devoted to nonclassical properties of light exhibited by sub-Poissonian photon statistics, negative reduced factorial moments or squeezing of quadrature variances below the coherent-state values. Statistical properties of modes involved in Raman or Brillouin processes have been studied for a long time (for reviews, see, e.g. [16, 17, 18]). Especially, results contained in papers [19, 20, 21], in which quantum statistical properties of Brillouin [19, 20] and Raman [21] processes were investigated in the framework of the generalized superposition of coherent fields and quantum noise, can be employed. The investigated model represents a generalization of the above models in the direction of incorporation of the influence of linear Stokes and anti-Stokes interactions.

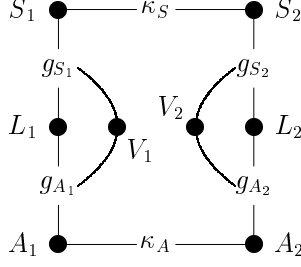


Figure 1: Scheme of interactions in the quantum nonlinear coupler formed from two nonlinear waveguides operating by means of Brillouin or Raman processes, in which Stokes and anti-Stokes modes mutually interact through evanescent waves; S_j , A_j , L_j , and V_j denote Stokes, anti-Stokes, laser pump, and phonon modes, g_{S_j} (g_{A_j}) is Stokes (anti-Stokes) nonlinear coupling constant in the j th waveguide, and κ_S (κ_A) represents Stokes (anti-Stokes) linear coupling constant.

Application of some earlier results for Raman scattering to obtain sum and difference squeezing of vacuum fluctuations were given in [22, 23], including the quantum correlations between the Stokes and anti-Stokes fields, whereas the correlations between the pump and Stokes waves were considered and measured in [24]. Raman effects can also play important role in quantum soliton propagation [25] and in solving various inverse scattering problems [26].

The dynamics of the couplers is solved analytically, numerically, and in a short-length approximation in Section 2. Quantum statistical properties of modes of the couplers are described in Section 3. Section 4 contains a discussion of the statistical behaviour of the systems under discussion based on results of the numerical analysis. Conclusions are summarized in Section 5.

2 Dynamics of nonlinear couplers

A model of the coupler composed of two mutually interacting waveguides with Raman or Brillouin processes is quantumly described by the following momentum operator (for a scheme of involved interactions, see Fig. 1):

$$\begin{aligned}
\hat{G} = & \sum_{j=L_1, S_1, A_1, V_1} \hbar k_j \hat{a}_j^\dagger \hat{a}_j + \left[\hbar \tilde{g}_{A_1} \hat{a}_{L_1} \hat{a}_{V_1} \hat{a}_{A_1}^\dagger + \hbar \tilde{g}_{S_1} \hat{a}_{L_1} \hat{a}_{V_1}^\dagger \hat{a}_{S_1} + \text{h.c.} \right] \\
& + \sum_{j=L_2, S_2, A_2, V_2} \hbar k_j \hat{a}_j^\dagger \hat{a}_j + \left[\hbar \tilde{g}_{A_2} \hat{a}_{L_2} \hat{a}_{V_2} \hat{a}_{A_2}^\dagger + \hbar \tilde{g}_{S_2} \hat{a}_{L_2} \hat{a}_{V_2}^\dagger \hat{a}_{S_2} + \text{h.c.} \right] \\
& + \left[\hbar \tilde{\kappa}_S \hat{a}_{S_1} \hat{a}_{S_2}^\dagger + \hbar \tilde{\kappa}_A \hat{a}_{A_1} \hat{a}_{A_2}^\dagger + \text{h.c.} \right], \tag{1}
\end{aligned}$$

where \hat{a}_j (\hat{a}_j^\dagger) are annihilation (creation) operators of laser (L), Stokes (S), anti-Stokes (A), and vibration (V) modes in the first (1) and the second (2) waveguides. Wave vectors of the corresponding modes are denoted as k_j . Coefficients \tilde{g}_{S_1} and \tilde{g}_{S_2} (\tilde{g}_{A_1} and \tilde{g}_{A_2}) describe nonlinear Stokes (anti-Stokes) interactions in the waveguides 1 and 2. Coefficients $\tilde{\kappa}_S$ and $\tilde{\kappa}_A$ are related to linear coupling between Stokes modes and anti-Stokes modes, respectively, in both the waveguides by means of the evanescent waves. The symbol \hbar denotes the reduced Planck constant and h.c. means Hermitian conjugate terms.

The momentum operator \hat{G} in (1) reflects a symmetry between the two waveguides, which is based on the exchange of the suffices (L_1, S_1, A_1, V_1) and the suffices (L_2, S_2, A_2, V_2) with the simultaneous exchange of constants $\tilde{\kappa}_S$, $\tilde{\kappa}_A$ with their complex conjugate ones $\tilde{\kappa}_S^*$, $\tilde{\kappa}_A^*$. This symmetry has to be conserved in spatial development of operators and all quantum statistical quantities, so we restrict our discussion of results only to modes in waveguide 1; results valid for waveguide 2 are obtained simply from the above mentioned symmetry.

Quantum spatial development of an operator \hat{a} is described by the Heisenberg equation $i\hbar \frac{d\hat{a}}{dz} = [\hat{G}, \hat{a}]$, where z is a spatial variable along the propagation direction, \hat{G} is the above introduced momentum operator and the symbol $[,]$ denotes a commutator. The Heisenberg equations for the operators \hat{A}_j in the interaction picture [$\hat{A}_j = \hat{a}_j \exp(-ik_j z)$] and under the assumption of strong classical laser pump modes L_1 and L_2 ($\hat{a}_j \rightarrow \alpha_j \exp(ik_j z)$ for $j = L_1, L_2$, α_j being classical amplitudes) have the form

$$\begin{aligned}\frac{d\hat{A}_{S_1}}{dz} &= ig_{S_1}\hat{A}_{V_1}^\dagger + i\kappa_S^*\hat{A}_{S_2}, \\ \frac{d\hat{A}_{A_1}}{dz} &= ig_{A_1}\hat{A}_{V_1} + i\kappa_A^*\hat{A}_{A_2}, \\ \frac{d\hat{A}_{V_1}}{dz} &= ig_{A_1}^*\hat{A}_{A_1} + ig_{S_1}\hat{A}_{S_1}^\dagger,\end{aligned}\tag{2}$$

where

$$\begin{aligned}g_{S_j} &= \tilde{g}_{S_j}\alpha_{L_j} \exp(i\Delta k_{S_j} z), \\ g_{A_j} &= \tilde{g}_{A_j}\alpha_{L_j} \exp(i\Delta k_{A_j} z), & \text{for } j = 1, 2, \\ \kappa_S &= \tilde{\kappa}_S \exp(i\Delta K_S z), \\ \kappa_A &= \tilde{\kappa}_A \exp(i\Delta K_A z)\end{aligned}\tag{3}$$

with the phase mismatch vectors $\Delta k_{S_j} = k_{L_j} - k_{V_j} - k_{S_j}$, $\Delta k_{A_j} = k_{L_j} + k_{V_j} - k_{A_j}$ for $j = 1, 2$ and $\Delta K_S = k_{S_1} - k_{S_2}$, $\Delta K_A = k_{A_1} - k_{A_2}$.

The Heisenberg equations (2) are linear, which enables us to solve them simply numerically and to retain operator character of the solution (see the next section). They can be also solved analytically under special conditions. Furthermore a short-length solution can be reached. These three kinds of solutions will be described in the following subsections.

The relation

$$\frac{d}{dz} \left[\sum_{j=1,2} \left(\hat{A}_{V_j}^\dagger(z)\hat{A}_{V_j}(z) + \hat{A}_{A_j}^\dagger(z)\hat{A}_{A_j}(z) - \hat{A}_{S_j}^\dagger(z)\hat{A}_{S_j}(z) \right) \right] = 0,\tag{4}$$

which represents a conservation law for photon numbers, can be derived directly from (2).

2.1 Numerical solution

The set of equations (2) can be conveniently written in the matrix form reflecting the symmetry of the model:

$$\begin{aligned}\frac{d\hat{\mathbf{A}}}{dz} &= i\hat{\mathbf{M}}\hat{\mathbf{A}}, \\ \hat{\mathbf{A}} &= \begin{bmatrix} \hat{\mathbf{A}}_1 \\ \hat{\mathbf{A}}_2 \end{bmatrix}, \hat{\mathbf{M}} = \begin{bmatrix} \hat{\mathbf{M}}_1 & \hat{\mathbf{M}}_{12} \\ \hat{\mathbf{M}}_{12}^* & \hat{\mathbf{M}}_2 \end{bmatrix},\end{aligned}\tag{5}$$

where the vectors $\hat{\mathbf{A}}_1$, $\hat{\mathbf{A}}_2$ and the matrices $\hat{\mathbf{M}}_1$, $\hat{\mathbf{M}}_2$, $\hat{\mathbf{M}}_{12}$ are defined as follows

$$\hat{\mathbf{A}}_j = \begin{bmatrix} \hat{A}_{S_j} \\ \hat{A}_{S_j}^\dagger \\ \hat{A}_{A_j} \\ \hat{A}_{A_j}^\dagger \\ \hat{A}_{V_j} \\ \hat{A}_{V_j}^\dagger \end{bmatrix},$$

$$\begin{aligned}
\hat{\mathbf{M}}_j &= \begin{bmatrix} 0 & 0 & 0 & 0 & 0 & g_{S_j} \\ 0 & 0 & 0 & 0 & -g_{S_j}^* & 0 \\ 0 & 0 & 0 & 0 & g_{A_j} & 0 \\ 0 & 0 & 0 & 0 & 0 & -g_{A_j}^* \\ 0 & g_{S_j} & g_{A_j}^* & 0 & 0 & 0 \\ -g_{S_j}^* & 0 & 0 & -g_{A_j} & 0 & 0 \end{bmatrix} & \text{for } j = 1, 2, \\
\hat{\mathbf{M}}_{12} &= \begin{bmatrix} \kappa_S^* & 0 & 0 & 0 & 0 & 0 \\ 0 & -\kappa_S & 0 & 0 & 0 & 0 \\ 0 & 0 & \kappa_A^* & 0 & 0 & 0 \\ 0 & 0 & 0 & -\kappa_A & 0 & 0 \\ 0 & 0 & 0 & 0 & 0 & 0 \\ 0 & 0 & 0 & 0 & 0 & 0 \end{bmatrix}. & (6)
\end{aligned}$$

The above set of equations is composed of two independent sets of equations for operators $(\hat{A}_{S_1}^\dagger, \hat{A}_{A_1}, \hat{A}_{V_1}, \hat{A}_{S_2}^\dagger, \hat{A}_{A_2}, \hat{A}_{V_2})$ and for their Hermitian conjugates. It is more convenient to manipulate with only one larger set of equations, because the procedure to solve them can be easily generalized for the case of losses in modes, in which also fluctuating Langevin forces must be taken into account; this results in coupling of operators and their conjugates through correlation functions of fluctuating forces (see, e.g. [27]).

Solution of equations (5) can be written in the form $\hat{\mathbf{A}}(z) = \exp(i\hat{\mathbf{M}}z)\hat{\mathbf{A}}(0)$ supposing that the matrix $\hat{\mathbf{M}}$ is z -independent. Since we assume in the following that all mismatches are zero, the matrix $\hat{\mathbf{M}}$ is really z -independent. Diagonalization of the matrix $\hat{\mathbf{M}}$ then enables us to determine spatial dependence of the evolution matrices \hat{U} and \hat{V} in the operator solution (for details, see e.g. [27])

$$\hat{A}_j(z) = \sum_{k=1}^6 \left[U_{jk}(z)\hat{A}_k(0) + V_{jk}(z)\hat{A}_k^\dagger(0) \right] \quad \text{for } j = 1, \dots, 6, \quad (7)$$

where the indices j, k run over the symbols $S_1, A_1, V_1, S_2, A_2,$ and V_2 .

2.2 Analytical solution

In a special case, characterized by the conditions

$$\begin{aligned}
|g_{S_1}| &= |g_{S_2}|, |g_{A_1}| = |g_{A_2}|, |\kappa_S| = |\kappa_A|, \\
\frac{\kappa_A^* g_{A_2}}{|\kappa_A| g_{A_1}} &= -\frac{\kappa_S g_{S_2}^*}{|\kappa_S| g_{S_1}^*}, & (8)
\end{aligned}$$

we can solve analytically the set of equations (5) using the following transformations ($\kappa = |\kappa_S|$):

$$\begin{aligned}
\hat{b}_S &= \frac{1}{\sqrt{2}} \exp(-i\kappa z) \left[\hat{A}_{S_1} + \frac{\kappa_S^*}{|\kappa_S|} \hat{A}_{S_2} \right], \\
\hat{c}_S &= \frac{1}{\sqrt{2}} \exp(i\kappa z) \left[\hat{A}_{S_1} - \frac{\kappa_S^*}{|\kappa_S|} \hat{A}_{S_2} \right], \\
\hat{b}_A &= \frac{1}{\sqrt{2}} \exp(-i\kappa z) \left[\hat{A}_{A_1} + \frac{\kappa_A^*}{|\kappa_A|} \hat{A}_{A_2} \right], \\
\hat{c}_A &= \frac{1}{\sqrt{2}} \exp(i\kappa z) \left[\hat{A}_{A_1} - \frac{\kappa_A^*}{|\kappa_A|} \hat{A}_{A_2} \right], \\
\hat{b}_V &= \frac{1}{\sqrt{2}} \exp(-i\kappa z) \left[\hat{A}_{V_1} + \frac{\kappa_A^* g_{A_2}}{|\kappa_A| g_{A_1}} \hat{A}_{V_2} \right], \\
\hat{c}_V &= \frac{1}{\sqrt{2}} \exp(i\kappa z) \left[\hat{A}_{V_1} - \frac{\kappa_A^* g_{A_2}}{|\kappa_A| g_{A_1}} \hat{A}_{V_2} \right]. & (9)
\end{aligned}$$

The application of the transformations (9) results in the following sets of equations:

$$\begin{aligned} \frac{d}{dz} \begin{bmatrix} \hat{b}_A \\ \hat{c}_S^\dagger \\ \hat{b}_V \end{bmatrix} &= i \begin{bmatrix} 0 & 0 & g_{A_1} \\ 0 & 0 & -g_{S_1}^* \\ g_{A_1}^* & g_{S_1} & -\kappa \end{bmatrix} \begin{bmatrix} \hat{b}_A \\ \hat{c}_S^\dagger \\ \hat{b}_V \end{bmatrix}, \\ \frac{d}{dz} \begin{bmatrix} \hat{c}_A \\ \hat{b}_S^\dagger \\ \hat{c}_V \end{bmatrix} &= i \begin{bmatrix} 0 & 0 & g_{A_1} \\ 0 & 0 & -g_{S_1}^* \\ g_{A_1}^* & g_{S_1} & \kappa \end{bmatrix} \begin{bmatrix} \hat{c}_A \\ \hat{b}_S^\dagger \\ \hat{c}_V \end{bmatrix} \end{aligned} \quad (10)$$

and two sets obtained by Hermitian conjugation of the above equations. These equations can be solved analytically (e.g. by finding eigenvalues and eigenvectors) and the inverse transformation leads to the solution of the operator equations (5) in the form:

$$\begin{aligned} \hat{A}_{S_1}(z) &= \frac{1}{r^2} \left[-|g_{A_1}|^2 \text{chh} + |g_{S_1}|^2 \left(-\frac{\kappa}{l^*} \text{sh sl}^* + \text{ch cl}^* \right) \right] \hat{A}_{S_1}(0) \\ &\quad + \frac{g_{A_1} g_{S_1}}{r^2} \left[-\text{chh} - \frac{\kappa}{l^*} \text{sh sl}^* + \text{ch cl}^* \right] \hat{A}_{A_1}^\dagger(0) \\ &\quad + i \frac{1}{r^2} \frac{\kappa_S^*}{|\kappa_S|} \left[-|g_{A_1}|^2 \text{shh} + |g_{S_1}|^2 \left(\frac{\kappa}{l^*} \text{ch sl}^* + \text{sh cl}^* \right) \right] \hat{A}_{S_2}(0) \\ &\quad + i \frac{g_{A_1} g_{S_1}}{r^2} \frac{\kappa_A}{|\kappa_A|} \left[\text{shh} - \frac{\kappa}{l^*} \text{ch sl}^* - \text{sh cl}^* \right] \hat{A}_{A_2}^\dagger(0) \\ &\quad + 2i \frac{g_{S_1}}{l^*} \text{ch sl}^* \hat{A}_{V_1}^\dagger(0) - 2 \frac{\kappa_S^*}{|\kappa_S|} \frac{g_{S_2}}{l^*} \text{sh sl}^* \hat{A}_{V_2}^\dagger(0), \\ \hat{A}_{A_1}(z) &= \frac{g_{A_1} g_{S_1}}{r^2} \left[\text{chh} + \frac{\kappa}{l} \text{sh sl} - \text{ch cl} \right] \hat{A}_{S_1}^\dagger(0) + 2i \frac{g_{A_1}}{l} \text{ch sl} \hat{A}_{V_1}(0) \\ &\quad + \frac{1}{r^2} \left[|g_{S_1}|^2 \text{chh} + |g_{A_1}|^2 \left(\frac{\kappa}{l} \text{sh sl} - \text{ch cl} \right) \right] \hat{A}_{A_1}(0) \\ &\quad + i \frac{1}{r^2} \frac{\kappa_A^*}{|\kappa_A|} \left[|g_{S_1}|^2 \text{shh} - |g_{A_1}|^2 \left(\frac{\kappa}{l} \text{ch sl} + \text{sh cl} \right) \right] \hat{A}_{A_2}(0) \\ &\quad - i \frac{g_{A_1} g_{S_1}}{r^2} \frac{\kappa_S}{|\kappa_S|} \left[\text{shh} - \frac{\kappa}{l} \text{ch sl} - \text{sh cl} \right] \hat{A}_{S_2}^\dagger(0) \\ &\quad - 2 \frac{\kappa_A^*}{|\kappa_A|} \frac{g_{A_2}}{l} \text{sh sl} \hat{A}_{V_2}(0), \\ \hat{A}_{V_1}(z) &= 2i \frac{g_{S_1}}{l} \text{ch sl} \hat{A}_{S_1}^\dagger(0) + 2i \frac{g_{A_1}}{l} \text{ch sl} \hat{A}_{A_1}(0) + \left[\frac{\kappa}{l} \text{sh sl} + \text{ch cl} \right] \hat{A}_{V_1}(0) \\ &\quad + 2 \frac{g_{S_1}}{l} \frac{\kappa_S}{|\kappa_S|} \text{sh sl} \hat{A}_{S_2}^\dagger(0) - 2 \frac{g_{A_1}}{l} \frac{\kappa_A^*}{|\kappa_A|} \text{sh sl} \hat{A}_{A_2}(0) \\ &\quad - i \frac{\kappa_A^*}{|\kappa_A|} \frac{g_{A_2}}{g_{A_1}} \left[\frac{\kappa}{l} \text{ch sl} - \text{sh cl} \right] \hat{A}_{V_2}(0). \end{aligned} \quad (11)$$

The abbreviations

$$\begin{aligned} \text{shh} &= \sin(\kappa z), & \text{chh} &= \cos(\kappa z), \\ \text{sh} &= \sin(\kappa z/2), & \text{ch} &= \cos(\kappa z/2), \\ \text{sl} &= \sin(lz/2), & \text{cl} &= \cos(lz/2), \\ r &= \sqrt{|g_{S_1}|^2 - |g_{A_1}|^2}, & l &= \sqrt{\kappa^2 - 4r^2} \end{aligned} \quad (12)$$

have been used in the above expressions. Expressions for operators \hat{A}_{S_2} , \hat{A}_{A_2} , and \hat{A}_{V_2} are obtained from the expressions (11) using the before mentioned symmetry of the coupler. Spatial development of creation operators follows from Hermitian conjugation of the expressions for annihilation operators.

2.3 Short-length solution

A short-length solution of equations (5) valid up to z^2 has the form:

$$\begin{aligned}
\hat{A}_{S_1}(z) &\approx \hat{A}_{S_1} + i \left(g_{S_1} \hat{A}_{V_1}^\dagger + \kappa_S^* \hat{A}_{S_2} \right) z \\
&\quad + \left(g_{S_1} g_{A_1} \hat{A}_{A_1}^\dagger + |g_{S_1}|^2 \hat{A}_{S_1} - \kappa_S^* g_{S_2} \hat{A}_{V_2}^\dagger - |\kappa_S|^2 \hat{A}_{S_1} \right) z^2/2 \\
\hat{A}_{A_1}(z) &\approx \hat{A}_{A_1} + i \left(g_{A_1} \hat{A}_{V_1} + \kappa_A^* \hat{A}_{A_2} \right) z \\
&\quad - \left(g_{S_1} g_{A_1} \hat{A}_{S_1}^\dagger + |g_{A_1}|^2 \hat{A}_{A_1} + \kappa_A^* g_{A_2} \hat{A}_{V_2} + |\kappa_A|^2 \hat{A}_{A_1} \right) z^2/2 \\
\hat{A}_{V_1}(z) &\approx \hat{A}_{V_1} + i \left(g_{A_1}^* \hat{A}_{A_1} + g_{S_1} \hat{A}_{S_1}^\dagger \right) z \\
&\quad - \left((|g_{A_1}|^2 - |g_{S_1}|^2) \hat{A}_{V_1} + g_{A_1}^* \kappa_A^* \hat{A}_{A_2} - g_{S_1} \kappa_S \hat{A}_{S_2}^\dagger \right) z^2/2.
\end{aligned} \tag{13}$$

Operators on the right hand sides of expressions in (13) are taken at $z = 0$. Expressions for the other operators are reached from the symmetry and by means of Hermitian conjugation of the above expressions.

3 Quantum statistical properties of nonlinear couplers

Quantum statistical properties of optical fields involved in the above processes can be studied in the framework of the generalized superposition of coherent fields and quantum noise ([18], Secs. 8.5, 9.3, and 9.4), which is characterized by the normal characteristic function $C_{\mathcal{N}}(\{\beta_j\}, z)$ in the Gaussian form:

$$\begin{aligned}
C_{\mathcal{N}}(\{\beta_j\}, z) &= \exp \left\{ \sum_{j=1}^6 \left[-B_j(z) |\beta_j|^2 + \left(\frac{1}{2} C_j(z) \beta_j^{*2} + \text{c.c.} \right) \right] \right. \\
&\quad + \sum_{j=1}^6 \sum_{k=1, j < k}^6 [D_{jk}(z) \beta_j^* \beta_k^* + \bar{D}_{jk}(z) \beta_j \beta_k + \text{c.c.}] \\
&\quad \left. + \sum_{j=1}^6 [\beta_j \xi_j^*(z) - \text{c.c.}] \right\},
\end{aligned} \tag{14}$$

where c.c. denotes the complex conjugate terms. The complex amplitudes $\xi_1(z), \dots, \xi_6(z)$ correspond to the annihilation operators $\hat{A}_{S_1}(z), \hat{A}_{A_1}(z), \hat{A}_{V_1}(z), \hat{A}_{S_2}(z), \hat{A}_{A_2}(z),$ and $\hat{A}_{V_2}(z)$, respectively. The quantum noise functions $B_j(z), C_j(z), D_{jk}(z),$ and $\bar{D}_{jk}(z)$ defined by the relations

$$\begin{aligned}
B_j(z) &= \langle \Delta \hat{A}_j^\dagger(z) \Delta \hat{A}_j(z) \rangle, \\
C_j(z) &= \langle (\Delta \hat{A}_j(z))^2 \rangle, \\
D_{jk}(z) &= \langle \Delta \hat{A}_j(z) \Delta \hat{A}_k(z) \rangle, \\
\bar{D}_{jk}(z) &= -\langle \Delta \hat{A}_j^\dagger(z) \Delta \hat{A}_k(z) \rangle,
\end{aligned} \tag{15}$$

can be determined in terms of values of these quantities for incident fields, B_j, C_j ($B_j = B_j(0) + 1, C_j = C_j(0)$ if antinormal ordering of field operators is adopted), provided that the operator solution of the corresponding Heisenberg equations is known (for details, see e.g. [28]). Antinormal ordering adopted for incident field operators enables us to describe nonclassical states of light. Values of quantities B_j and C_j are given in the case of the squeezed fields with additional noise by

$$\begin{aligned}
B_j &= \cosh^2(r_j) + \langle n_{chj} \rangle, \\
C_j &= \frac{1}{2} \exp(i\theta_j) \sinh(2r_j),
\end{aligned} \tag{16}$$

where r_j are the squeeze parameters of the incident beams, θ_j are the squeeze phases and $\langle n_{chj} \rangle$ represent the mean number of external noise particles in the j th mode. In general signal squeezed light with an additional noise is described by the above expressions; when $r_j = 0$, $\langle n_{chj} \rangle = 0$ ($B_j = 1$, $C_j = 0$) we have a coherent state and the superposition of the signal coherent field and noise is characterized by $r_j = 0$, $\langle n_{chj} \rangle \neq 0$ ($B_j = \langle n_{chj} \rangle + 1$, $C_j = 0$).

The photon number distribution $p(n_j, z)$ and the moments of the integrated intensity $\langle W_j^k(z) \rangle$ can be obtained from the normal characteristic function $C_{\mathcal{N}}(\beta_j, z)$ given in (14) in terms of the Laguerre polynomials for both single and compound (two-mode) fields (for details, see e.g. [8, 18, 28] and references therein). Expressions for variances of quadrature components $\langle (\Delta \hat{p}_j(z))^2 \rangle$, $\langle (\Delta \hat{q}_j(z))^2 \rangle$, for principal squeeze variance $\lambda_j(z)$, and for uncertainty product $u_j(z)$ can also be found in [8, 18, 28].

We introduce only expressions for the variances $\langle (\Delta W)^2 \rangle$ of the integrated intensity and for the principal squeeze variances λ for single and compound modes, which will be used when analyzing the statistical properties on the basis of the short-length solution.

We get the variance $\langle (\Delta W_j)^2 \rangle$ of the integrated intensity in the form ([18], p. 268)

$$\langle [\Delta W_j(z)]^2 \rangle = B_j^2(z) + |C_j(z)|^2 + 2B_j(z)|\xi_j(z)|^2 + (C_j(z)\xi_j^{*2}(z) + \text{c.c.}) \quad (17)$$

for the j th single mode. The variance of the integrated intensity of the (j, k) th compound mode equals

$$\langle [\Delta W_{jk}(z)]^2 \rangle = \langle [\Delta W_j(z)]^2 \rangle + \langle [\Delta W_k(z)]^2 \rangle + 2\langle \Delta W_j(z)\Delta W_k(z) \rangle, \quad (18)$$

where the correlation of fluctuations of integrated intensities is given by

$$\begin{aligned} \langle \Delta W_j(z)\Delta W_k(z) \rangle &= |D_{jk}(z)|^2 + |\bar{D}_{jk}(z)|^2 \\ &+ (D_{jk}(z)\xi_j^*(z)\xi_k^*(z) - \bar{D}_{jk}(z)\xi_j(z)\xi_k^*(z) + \text{c.c.}). \end{aligned} \quad (19)$$

The principal squeeze variances $\lambda_j(z)$ for the j th single mode and $\lambda_{jk}(z)$ for the (j, k) th compound mode are expressed as [8]:

$$\begin{aligned} \lambda_j(z) &= 1 + 2[B_j(z) - |C_j(z)|], \\ \lambda_{jk}(z) &= 2\{1 + B_j(z) + B_k(z) - (\bar{D}_{jk}(z) + \text{c.c.}) \\ &\quad - |C_j(z) + C_k(z) + 2D_{jk}(z)|\}. \end{aligned} \quad (20)$$

We now can pay our attention to the statistical properties of the short-length solution. We firstly discuss the case with all modes being at the beginning of the interaction in coherent states (Brillouin processes). The coefficients of the normal characteristic function $C_{\mathcal{N}}(\{\beta_j\}, z)$ read up to z^2 :

$$\begin{aligned} B_{S_1}(z) &= |g_{S_1}|^2 z^2, \\ B_{V_1}(z) &= |g_{S_1}|^2 z^2, \\ D_{S_1 A_1}(z) &= -g_{A_1} g_{S_1} z^2 / 2, \\ D_{S_1 V_1}(z) &= i g_{S_1} z, \\ D_{S_1 V_2}(z) &= -g_{S_2} \kappa_S^* z^2 / 2. \end{aligned} \quad (21)$$

The other coefficients (not obtained from the symmetry) are zero. We get from (17) and (21) for single mode variances of the integrated intensity

$$\begin{aligned} \langle (\Delta W_{S_1}(z))^2 \rangle &= 2|g_{S_1}|^2 |\xi_{S_1}|^2 z^2, \\ \langle (\Delta W_{A_1}(z))^2 \rangle &= 0, \\ \langle (\Delta W_{V_1}(z))^2 \rangle &= 2|g_{S_1}|^2 |\xi_{V_1}|^2 z^2. \end{aligned} \quad (22)$$

The symbols ξ denote initial coherent amplitudes of the radiation and phonon modes. The variances of the integrated intensity for compound modes, which can be negative, read

$$\begin{aligned}
\langle(\Delta W_{S_1 A_1}(z))^2\rangle &= 2|g_{S_1}|^2|\xi_{S_1}|^2 z^2 - (g_{A_1} g_{S_1} \xi_{S_1}^* \xi_{A_1}^* z^2 + \text{c.c.}), \\
\langle(\Delta W_{S_1 V_1}(z))^2\rangle &= 2[(i g_{S_1} \xi_{S_1}^* \xi_{V_1}^* z + \text{c.c.}) + |g_{S_1}|^2(1 + 3|\xi_{S_1}|^2 + 3|\xi_{V_1}|^2) z^2 \\
&\quad + (g_{S_1} g_{A_1} \xi_{A_1}^* \xi_{S_1}^* z^2 + \text{c.c.}) + (g_{S_1} \kappa_S \xi_{S_2}^* \xi_{V_1}^* z^2 + \text{c.c.})], \\
\langle(\Delta W_{S_1 V_2}(z))^2\rangle &= 2|g_{S_1}|^2|\xi_{S_1}|^2 z^2 + 2|g_{S_2}|^2|\xi_{V_2}|^2 z^2 - (g_{S_2} \kappa_S^* \xi_{S_1}^* \xi_{V_2}^* z^2 + \text{c.c.}).
\end{aligned} \tag{23}$$

From the point of view of the short-length solution, negative variances of the integrated intensity reflecting nonclassical properties of light can be reached only in the compound modes (S_1, A_1) , (S_1, V_1) , and (S_1, V_2) when initial phases are suitably chosen. The linear coupling between Stokes modes (described by κ_S) leads to the negative integrated intensity variance in the compound mode (S_1, V_2) and it also can support the negative integrated intensity variance of the mode (S_1, V_1) .

The coefficients $C_j(z)$ are zero not only in the short-length solution but also when we suppose initial non-squeezed light ($C_j(0) = 0$). This stems from the momentum operator (1), which contains only first powers of operators. This excludes squeezing in single mode fields. Squeezing of vacuum fluctuations can be reached in the compound modes (S_1, A_1) , (S_1, V_1) , and (S_1, V_2) , the principal squeeze variances of which are given by, using (20) and (21):

$$\begin{aligned}
\lambda_{S_1 A_1}(z) &= 2[1 + |g_{S_1}|(|g_{S_1}| - |g_{A_1}|)z^2], \\
\lambda_{S_1 V_1}(z) &= 2[1 - 2|g_{S_1}|z + |g_{S_1}|^2 z^2], \\
\lambda_{S_1 V_2}(z) &= 2[1 + (|g_{S_1}|^2 + |g_{S_2}|^2)z^2 - |g_{S_2}||\kappa_S|z^2].
\end{aligned} \tag{24}$$

The linear Stokes coupling κ_S thus can lead to generation of squeezed light in the mode (S_1, V_2) .

Now using the short-length solution we analyze statistical properties of modes for Raman processes, i.e. when phonons are initially chaotic and the other modes are initially coherent. Coefficients in the normal characteristic function $C_{\mathcal{N}}(\{\beta_j\}, z)$ have the form:

$$\begin{aligned}
B_{S_1}(z) &= |g_{S_1}|^2(n_{V_1} + 1)z^2, \\
B_{A_1}(z) &= |g_{A_1}|^2 n_{V_1} z^2, \\
B_{V_1}(z) &= n_{V_1} + |g_{S_1}|^2(n_{V_1} + 1)z^2 - |g_{A_1}|^2 n_{V_1} z^2, \\
D_{S_1 A_1}(z) &= -g_{S_1} g_{A_1} (n_{V_1} + 1/2)z^2, \\
D_{S_1 V_1}(z) &= i g_{S_1} (n_{V_1} + 1)z, \\
D_{S_1 V_2}(z) &= -g_{S_2} \kappa_S^* (n_{V_2} + 1)z^2/2, \\
\bar{D}_{A_1 V_1}(z) &= i g_{A_1}^* n_{V_1} z, \\
\bar{D}_{A_1 V_2}(z) &= g_{A_2}^* \kappa_A n_{V_2} z^2/2.
\end{aligned} \tag{25}$$

The other coefficients, which are not obtained from the symmetry, are zero. The mean numbers of initial chaotic phonons are denoted as n_{V_1} and n_{V_2} for modes V_1 and V_2 , respectively.

Variances of the integrated intensity for both single and compound modes can be expressed using relations (17), (18) and (25):

$$\begin{aligned}
\langle(\Delta W_{S_1}(z))^2\rangle &= 2|g_{S_1}|^2(n_{V_1} + 1)|\xi_{S_1}|^2 z^2, \\
\langle(\Delta W_{A_1}(z))^2\rangle &= 2|g_{A_1}|^2 n_{V_1} |\xi_{A_1}|^2 z^2, \\
\langle(\Delta W_{V_1}(z))^2\rangle &= n_{V_1}^2 + 2|g_{S_1}|^2 n_{V_1} (|\xi_{S_1}|^2 + n_{V_1} + 1)z^2 \\
&\quad + 2|g_{A_1}|^2 n_{V_1} (|\xi_{A_1}|^2 - n_{V_1})z^2 + (2g_{A_1}^* g_{S_1}^* \xi_{S_1} \xi_{A_1} n_{V_1} + \text{c.c.}), \\
\langle(\Delta W_{S_1 A_1}(z))^2\rangle &= 2|g_{S_1}|^2(n_{V_1} + 1)|\xi_{S_1}|^2 z^2 + 2|g_{A_1}|^2 n_{V_1} |\xi_{A_1}|^2 z^2 \\
&\quad - [g_{A_1} g_{S_1} (2n_{V_1} + 1) \xi_{S_1}^* \xi_{A_1}^* z^2 + \text{c.c.}], \\
\langle(\Delta W_{S_1 V_1}(z))^2\rangle &= n_{V_1}^2 + 2|g_{S_1}|^2(3|\xi_{S_1}|^2 + n_{V_1} + 1)(n_{V_1} + 1)z^2
\end{aligned}$$

$$\begin{aligned}
& + [2g_{A_1}g_{S_1}(n_{V_1} + 1)\xi_{S_1}^*\xi_{A_1}^*z^2 + \text{c.c.}], \\
\langle(\Delta W_{A_1V_1}(z))^2\rangle & = n_{V_1}^2 + 2|g_{A_1}|^2n_{V_1}(n_{V_1} - |\xi_{A_1}|^2)z^2 \\
& - [2g_{A_1}g_{S_1}n_{V_1}\xi_{S_1}^*\xi_{A_1}^*z^2 + \text{c.c.}].
\end{aligned} \tag{26}$$

The above short-length expressions (26) indicate negative variances of the integrated intensity only in the compound mode (S_1, A_1) . The influence of linear Stokes (κ_S) and anti-Stokes (κ_A) couplings on the variances cannot be deduced from the expressions restricted up to z^2 .

As has been discussed previously, squeezing of vacuum fluctuations cannot be obtained in single modes. However, the short-length solution provides interesting results for principal squeeze variances of the following compound modes, using (20) and (25):

$$\begin{aligned}
\lambda_{S_1A_1}(z) & = 2[1 + |g_{S_1}|^2(n_{V_1} + 1)z^2 + |g_{A_1}|^2n_{V_1}z^2 - |g_{A_1}||g_{S_1}|(1 + 2n_{V_1})z^2], \\
\lambda_{S_1V_1}(z) & = 2[1 + n_{V_1} - 2|g_{S_1}|(n_{V_1} + 1)z + 2|g_{S_1}|^2(n_{V_1} + 1)z^2 - |g_{A_1}|^2n_{V_1}z^2], \\
\lambda_{A_1V_1}(z) & = 2[1 + n_{V_1} - (ig_{A_1}^*n_{V_1}z + \text{c.c.}) + |g_{S_1}|^2(n_{V_1} + 1)z^2], \\
\lambda_{S_1V_2}(z) & = 2[1 + n_{V_2} + |g_{S_1}|^2(n_{V_1} + 1)z^2 + |g_{S_2}|^2(n_{V_2} + 1)z^2 - |g_{A_2}|^2n_{V_2}z^2 \\
& - |g_{S_2}|\kappa_S|(n_{V_2} + 1)z^2], \\
\lambda_{A_1V_2}(z) & = 2[1 + n_{V_2} + |g_{S_2}|^2(n_{V_2} + 1)z^2 + |g_{A_1}|^2n_{V_1}z^2 - |g_{A_2}|^2n_{V_2}z^2 \\
& - (g_{A_2}^*\kappa_A n_{V_2}z^2 + \text{c.c.})].
\end{aligned} \tag{27}$$

Thus, squeezing can be reached in mode (S_1, A_1) for small n_{V_1} . Especially, the above expressions show that Stokes linear coupling (κ_S) could generate squeezing in mode (S_1, V_2) and anti-Stokes linear coupling (κ_A) could lead to squeezing in mode (A_1, V_2) .

The advantage of the short-length solutions stems from their simpler expressions which can be relatively easily analyzed. The relations above introduced enable us to reveal partly the role of Stokes and anti-Stokes coupling constants in generation of light with nonclassical properties. As it will be seen in the next section, the dynamics of the statistical properties is more complex in general than it may be seen in the short-length solution; but all tendencies are obvious from the short-length solution. The short-length solution is important especially for understanding the role of various initial phases, which can substantially change the statistical behaviour of nonlinear couplers.

4 Statistical behaviour of nonlinear couplers

This section contains a discussion of the statistical behaviour of the Raman and Brillouin couplers obtained on the basis of numerical results gained by applying the method described in section 2.1. In special cases, analytical solution from section 2.2 can be used to verify the correctness of the numerical approach. The discussion further generalizes results obtained in the previous section by means of the short-length solution. The couplers with Brillouin and Raman processes in operation will be discussed separately.

Photon number distribution $p(n_j, z)$, reduced moments of the integrated intensity $\langle W^k(z) \rangle / \langle W(z) \rangle^k - 1$, variances of quadrature components $\langle (\Delta \hat{p}_j(z))^2 \rangle$, $\langle (\Delta \hat{q}_j(z))^2 \rangle$, principal squeeze variance $\lambda_j(z)$, and the uncertainty product parameter $u_j(z)$ (for definitions, see [8]) will be used when discussing the statistical properties of single and compound modes. Nonclassical behaviour of a field exhibits itself by sub-Poissonian photon number statistics, by negative reduced moments of the integrated intensity (they indicate antibunching of photons; a field with negative second reduced moment of the integrated intensity possesses a sub-Poissonian statistics) or by squeezing of quadrature variances (the variance is squeezed if its value is under 1 (2) for a single (compound) mode).

Squeezing of vacuum fluctuations and sub-Poissonian statistics cannot be reached in single modes, if the fields are initially in coherent states or in coherent states with superimposed noise (this is connected with the fact that the coefficients $C_j(z)$ in the normal characteristic function

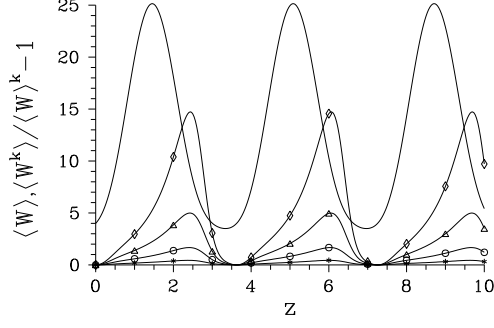


Figure 2: Mean integrated intensity $\langle W(z) \rangle$ (solid curve without denotation) and reduced moments of the integrated intensity $\langle W^k(z) \rangle / \langle W(z) \rangle^k - 1$ for $k = 2(*)$, $k = 3(o)$, $k = 4(\Delta)$, and $k = 5(\diamond)$ for mode (S_1, A_1) ; $g_{S_1} = 1$, $g_{A_1} = 2$, $\xi_{S_1} = 2i$, $\xi_{V_1} = 1$, and the other parameters are zero.

(14) are zero provided that they are initially zero). That is why we orientate our attention mainly to two-mode fields.

We choose the condition $|g_A| > |g_S|$ in cases discussed below, because such a condition is suitable for nonclassical light generation [19, 20].

4.1 Coupler with Brillouin processes

We suppose initial coherent states in all six modes of the coupler. We divide the discussion to six sections; in each section a special configuration is discussed. These configurations change from simpler to more complex ones.

Influence of κ_S on stimulated Stokes process

We suppose stimulated Stokes and spontaneous anti-Stokes processes in waveguide 1 ($g_{S_1} \neq 0$, $g_{A_1} \neq 0$, $\xi_{S_1} \neq 0$, $\xi_{V_1} \neq 0$, $\xi_{A_1} = 0$). Reduced moments of the integrated intensity (in the following we simply speak of moments of intensity) for compound mode (S_1, V_1) can be negative if phases are suitably chosen (see the short-length solution (23)). Moments of intensity in modes (S_1, A_1) and (A_1, V_1) are non-negative. Squeezing can be reached in modes (S_1, A_1) and (S_1, V_1) . There is a periodicity in the spatial development with the period $1/\sqrt{|g_{A_1}|^2 - |g_{S_1}|^2}$ (see [19]). Single and compound modes return periodically to coherent states (see Fig. 2 for mode (S_1, A_1)).

The introduction of the linear Stokes coupling ($\kappa_S \neq 0$, $\xi_{S_2} \neq 0$) leads to the occurrence of negative moments of intensity also in modes (S_1, A_1) (see Fig. 3a, compare it with Fig. 2), (S_2, V_1) , and (S_2, A_1) . Fig. 3b illustrates a typical spatial development of the photon number distribution of compound modes with negative moments of intensity: the initially Poissonian statistics develop to regions exhibiting sub-Poissonian statistics in interchange with regions exhibiting super-Poissonian statistics. Squeezing of vacuum fluctuations can be reached also in modes (S_2, V_1) and (S_2, A_1) (see Fig. 3c for mode (S_2, A_1)). The increase of κ_S decreases the period of the spatial dynamics (as indicated by the analytical solution in (11)) and it does not lead to an increase of noise for longer z , but to a tendency to conserve the initial statistics.

The introduction of the Stokes process in waveguide 2 ($g_{S_2} \neq 0$, $\xi_{V_2} \neq 0$) does not lead to nonclassical properties of mode (V_1, V_2) at all.

Influence of κ_A on stimulated anti-Stokes process

We suppose stimulated anti-Stokes and spontaneous Stokes processes in waveguide 1 ($g_{S_1} \neq 0$, $g_{A_1} \neq 0$, $\xi_{A_1} \neq 0$, $\xi_{V_1} \neq 0$, $\xi_{S_1} = 0$). Negative moments of intensity can be reached in mode (S_1, A_1) if the initial phase of ξ_{A_1} is suitably chosen ($\arg(\xi_{A_1}) = \pm\pi/2$). Squeezing in modes (S_1, A_1) and (S_1, V_1) reflects nonclassical properties of fields in this case. Non-zero anti-Stokes

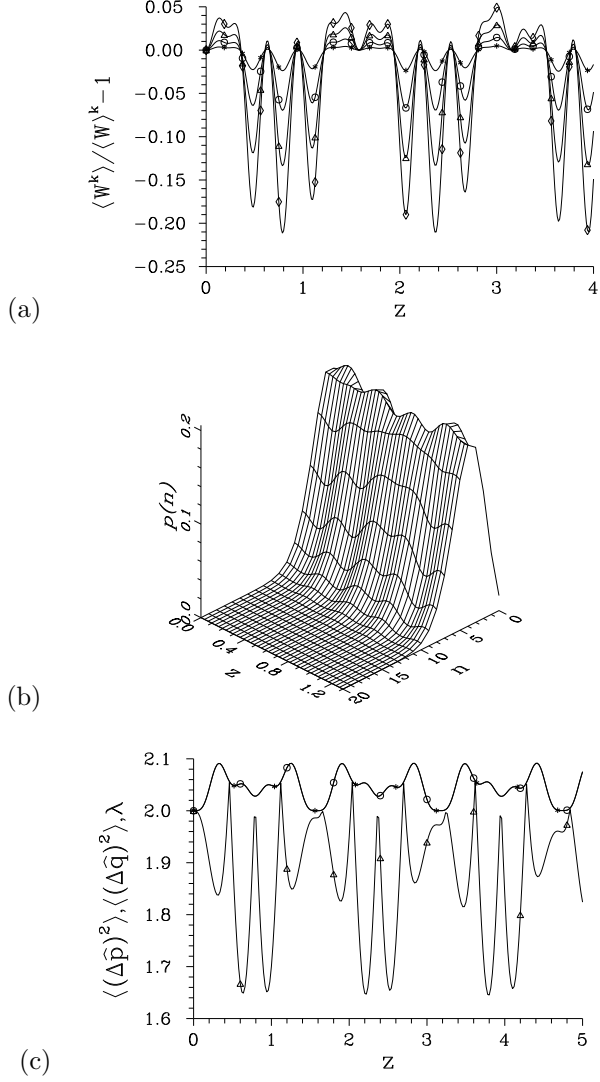


Figure 3: Reduced moments of the integrated intensity $\langle W^k(z) \rangle / \langle W(z) \rangle^k - 1$ for $k = 2$ (*), $k = 3$ (o), $k = 4$ (Δ), and $k = 5$ (\diamond) for mode (S_1, A_1) **(a)**, photon number distribution $p(n, z)$ for mode (S_1, A_1) **(b)**, and quadrature variances $\langle (\Delta \hat{p}(z))^2 \rangle$ (*), $\langle (\Delta \hat{q}(z))^2 \rangle$ (o), and principal squeeze variance $\lambda(z)$ (Δ) **(c)** for mode (S_2, A_1) ; $g_{S_1} = 1$, $g_{A_1} = 2$, $\kappa_S = -10$, $\xi_{S_1} = 2$, $\xi_{V_1} = 1$, $\xi_{S_2} = 2$, and the other parameters are zero.

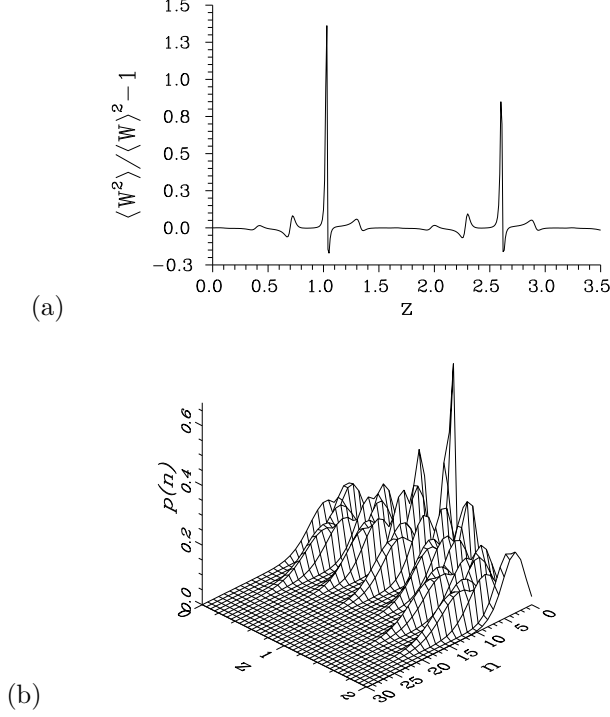


Figure 4: The second reduced moment of the integrated intensity $\langle W^2(z) \rangle / \langle W(z) \rangle^2 - 1$ **(a)** and the photon number distribution $p(n, z)$ for mode (S_2, A_1) **(b)**; $g_{S_1} = 1$, $g_{A_1} = 2$, $\kappa_S = -10$, $\xi_{S_1} = -2i$, $\xi_{A_1} = 2i$, $\xi_{V_1} = 1$, $\xi_{S_2} = 2$, and the other parameters are zero.

coupling ($\kappa_A \neq 0$, $\xi_{A_2} \neq 0$) does not support nonclassical properties, but it can lead to transmission of light exhibiting negative moments of intensity from mode (S_1, A_1) to mode (S_1, A_2) . Non-zero κ_A causes a fast increase of mean intensity and its moments. Faster oscillations in z occur in the spatial development of discussed quantities, but they are connected with a gradual increase of noise. There occur periods with a noise reduction. The coupling constant κ_A destroys gradually squeezing in modes (S_1, A_1) and (S_1, V_1) .

Influence of κ_S on stimulated Stokes and anti-Stokes processes

Stimulated Stokes and anti-Stokes processes in waveguide 1 are assumed ($g_{S_1} \neq 0$, $g_{A_1} \neq 0$, $\xi_{S_1} \neq 0$, $\xi_{A_1} \neq 0$, $\xi_{V_1} \neq 0$). Negative moments of intensity and squeezing occur in both modes (S_1, A_1) and (S_1, V_1) if phases are suitably chosen ($\phi_V + \phi_S - \phi_{g_S} = -\pi/2$, $\phi_V - \phi_A + \phi_{g_A} = -\pi/2$, see [19]).

The interaction of mode S_2 through Stokes coupling ($\kappa_S \neq 0$, $\xi_{S_2} \neq 0$) leads to the occurrence of negative moments of the intensity and to squeezing also in modes (S_2, A_1) (see Figs. 4a and 4b) and (S_2, V_1) . Fig. 4b demonstrates photon number distribution $p(n, z)$ for mode (S_2, A_1) , which exhibits oscillations between sub-Poissonian and super-Poissonian statistics when z increases (compare Fig. 4b with Fig. 4a).

If the phases are not suitably chosen, moments of mode (S_1, A_1) are non-negative when the Stokes coupling is not included ($\kappa_S = 0$) ($\phi_V + \phi_S - \phi_{g_S} = -\pi/2$, $\phi_V - \phi_A + \phi_{g_A} = \pi/2$, see [19]). The inclusion of the Stokes coupling can stimulate negative moments of intensity in this mode.

The addition of stimulated Stokes process in waveguide 2 ($g_{S_2} \neq 0$, $\xi_{S_2} \neq 0$) does not lead to negative moments of intensity in mode (V_1, V_2) .

Influence of κ_A on stimulated Stokes and anti-Stokes processes

Non-zero anti-Stokes coupling ($\kappa_A \neq 0$, $\xi_{A_2} \neq 0$) of waveguide 2 suppresses nonclassical behaviour of compound modes in waveguide 1 ($g_{S_1} \neq 0$, $g_{A_1} \neq 0$, $\xi_{S_1} \neq 0$, $\xi_{A_1} \neq 0$, $\xi_{V_1} \neq 0$) for longer z . It introduces oscillations to the spatial development of quantities under investigation and it increases noise in moments of intensity and supports higher values of quadrature variances. However, negative moments of intensity and squeezing for shorter z can be reached in mode (S_1, A_2) as a consequence of the linear anti-Stokes coupling.

The anti-Stokes process in waveguide 2 ($g_{A_2} \neq 0$, $\xi_{V_2} \neq 0$) does not create nonclassical effects in compound modes (A_1, A_2) , (A_2, V_1) , (A_1, V_2) , (V_1, V_2) , and (S_1, V_2) .

Influence of κ_S on stimulated Stokes and anti-Stokes processes in both waveguides

Stimulated Stokes and anti-Stokes processes in both the waveguides are assumed now ($g_{S_1} \neq 0$, $g_{A_1} \neq 0$, $\xi_{S_1} \neq 0$, $\xi_{A_1} \neq 0$, $\xi_{V_1} \neq 0$, $g_{S_2} \neq 0$, $g_{A_2} \neq 0$, $\xi_{S_2} \neq 0$, $\xi_{A_2} \neq 0$, $\xi_{V_2} \neq 0$). Negative moments of intensity and squeezing occur in compound modes (S_1, A_1) , (S_1, V_1) , (S_2, A_2) , and (S_2, V_2) when phases are suitably chosen. The linear Stokes coupling ($\kappa_S \neq 0$) conserves slightly negative moments of intensity and squeezing in these modes (see Fig. 5a for mode (S_1, A_1)) and it can induce negative moments of intensity and squeezing also in compound modes composed of single modes in different waveguides, especially in modes (S_2, A_1) , (S_2, V_1) , (S_1, A_2) , and (S_1, V_2) (see Fig. 5b for mode (S_2, V_1) ; in mode (S_1, A_2) substantial squeezing of vacuum fluctuations can be obtained). The dynamics of the mean intensity and of moments in Fig. 5a shows a typical behaviour of compound modes; regions with slightly negative moments are followed by short regions of high increase of noise, when a decrease of the mean intensity changes to an increase. Complex values of κ_S introduce asymmetry between the waveguides, which affects strongly the spatial development of the compound modes.

Negative moments of intensity or squeezing are not generated in compound modes constituted by the same single modes in different waveguides, i.e. in modes (S_1, S_2) , (A_1, A_2) , and (V_1, V_2) (see Fig. 5c for mode (A_1, A_2)). However, these modes possess strong tendency to return to the coherent states.

Influence of Stokes and anti-Stokes couplings on Brillouin processes in both waveguides

Now we discuss a general configuration, i.e. we extend the configuration from the previous part by including anti-Stokes coupling ($\kappa_A \neq 0$). Nonclassical effects in compound modes occur for the same modes, as discussed in the previous section, when values of the coupling constant κ_A were small. The increase of values of κ_A causes a successive increase of moments of intensity for both modes with negative moments (see Figs. 6a and 6b for mode (S_2, A_1)) and modes with non-negative moments. This means that the occurrence of negative moments of intensity is restricted to shorter z for greater κ_A (compare Figs. 6a and 6b) or negative moments cannot occur at all.

Greater values of κ_A mostly lead to a successive increase of values of variances and uncertainty product, but they can also serve to generate light, squeezing of which gradually develops with z (see Fig. 6c for mode (S_1, A_1)).

If we compare the above results with the short-length ones, we can conclude that the general solution reveals richer possibilities for nonclassical light generation. The short-length solution together with the analytical one [19] are extremely important for a suitable choice of phases, which are crucial for the generation of nonclassical light, as can be deduced from the short-length solution in the previous section.

4.2 Coupler with Raman processes

Initial coherent states in optical modes (Stokes, anti-Stokes) and initial chaotic states in phonon modes are assumed in the following discussion, which is again divided into the same six sections, as was done in the case of Brillouin processes. In general, the occurrence of regimes giving nonclassical effects in the statistical behaviour of light is similar as in the case of Brillouin processes. However,

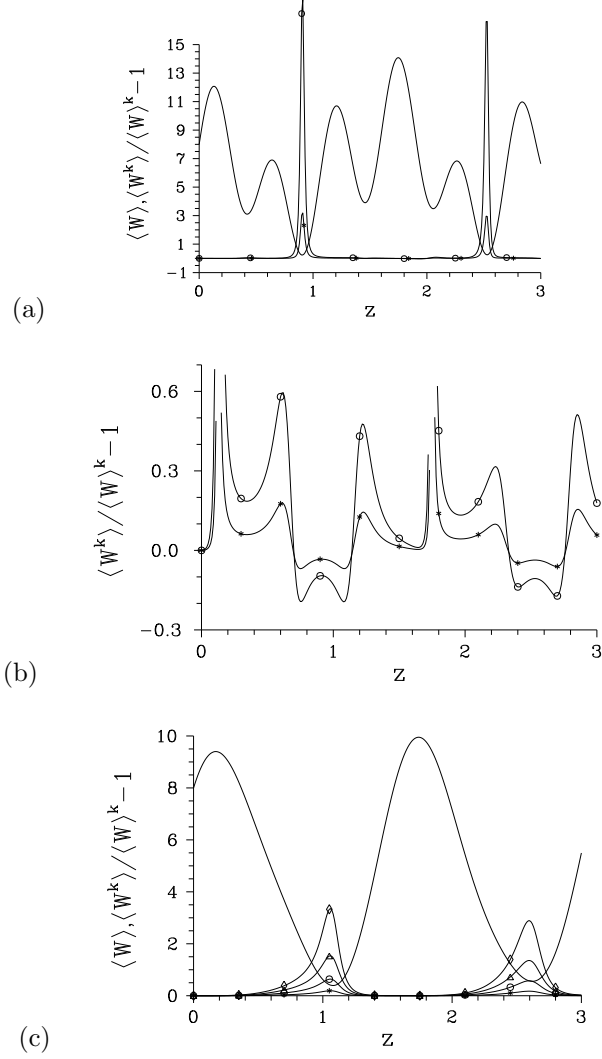


Figure 5: Mean integrated intensity $\langle W(z) \rangle$ (solid curve without denotation) and reduced moments of the integrated intensity $\langle W^k(z) \rangle / \langle W(z) \rangle^k - 1$ for $k = 2$ (*) and $k = 3$ (o) for mode (S_1, A_1) **(a)**, reduced moments of the integrated intensity $\langle W^k(z) \rangle / \langle W(z) \rangle^k - 1$ for $k = 2$ (*) and $k = 3$ (o) for mode (S_2, V_1) **(b)**, and mean integrated intensity $\langle W(z) \rangle$ (solid curve without denotation) and reduced moments of the integrated intensity $\langle W^k(z) \rangle / \langle W(z) \rangle^k - 1$ for $k = 2$ (*), $k = 3$ (o), $k = 4$ (Δ), and $k = 5$ (\diamond) for mode (A_1, A_2) **(c)**; $g_{S_1} = 1$, $g_{A_1} = 2$, $\kappa_S = 6i$, $g_{S_2} = 1$, $g_{A_2} = 2$, $\xi_{S_1} = -2i$, $\xi_{A_1} = 2i$, $\xi_{V_1} = 1$, $\xi_{S_2} = -2i$, $\xi_{A_2} = 2i$, $\xi_{V_2} = 1$, and the other parameters are zero.

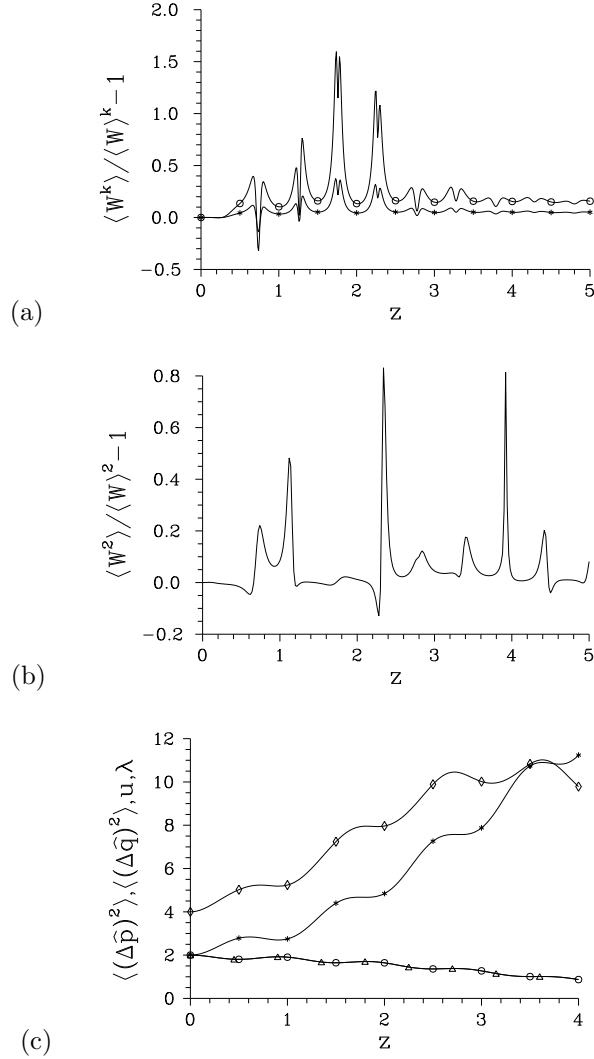


Figure 6: Reduced moments of the integrated intensity $\langle W^k(z) \rangle / \langle W(z) \rangle^k - 1$ for $k = 2$ (*) and $k = 3$ (o) for mode (S_2, A_1) **(a)**, the second reduced moment of the integrated intensity $\langle W^2(z) \rangle / \langle W(z) \rangle^2 - 1$ for mode (S_2, A_1) ($\kappa_A = i$) **(b)**, and quadrature variances $\langle (\Delta \hat{p}(z))^2 \rangle$ (*), $\langle (\Delta \hat{q}(z))^2 \rangle$ (o), principal squeeze variance $\lambda(z)$ (Δ), and uncertainty product $u(z)$ (\diamond) for mode (S_1, A_1) **(c)**; $\kappa_A = 6i$ and the other parameters are the same as in Fig. 5.

one can expect a diminished role of various phase relations for the occurrence of nonclassical light, owing to chaotic statistics of phonon modes, compared with the above discussed case. The short-length solution provides less information in this case.

Influence of κ_S on stimulated Stokes process

Stimulated Stokes process ($g_{S_1} \neq 0$, $g_{A_1} \neq 0$, $\xi_{S_1} \neq 0$, $n_{V_1} \neq 0$) supports the squeezed light generation in compound modes (S_1, A_1) and (S_1, V_1) . Non-zero Stokes coupling ($\kappa_S \neq 0$, $\xi_{S_2} \neq 0$) supports nonclassical light generation. Especially, it induces antibunching in modes (S_1, A_1) , (S_1, V_1) , (S_2, A_1) , and (S_2, V_1) and also squeezing in modes (S_2, A_1) and (S_2, V_1) . The increase of values of n_{V_1} destroys antibunching in all modes. Antibunching in modes (S_2, A_1) and (S_2, V_1) disappears for smaller n_{V_1} .

Influence of κ_A on stimulated anti-Stokes process

Squeezed light in compound modes (S_1, A_1) and (S_1, V_1) can be generated in stimulated anti-Stokes process ($g_{S_1} \neq 0$, $g_{A_1} \neq 0$, $\xi_{A_1} \neq 0$, $n_{V_1} \neq 0$). If values of mean phonon number n_{V_1} are small, antibunching in mode (S_1, A_1) occurs. In this case, anti-Stokes coupling ($\kappa_A \neq 0$, $\xi_{A_2} \neq 0$) leads to transmission of antibunching to mode (S_1, A_2) . The anti-Stokes linear coupling supports also squeezing in mode (S_1, A_2) . However, antibunching and squeezing can occur only provided that n_{V_1} is sufficiently small.

Influence of κ_S on stimulated Stokes and anti-Stokes processes

Negative moments of intensity in mode (S_1, A_1) and squeezing in modes (S_1, A_1) and (S_1, V_1) characterize nonclassical properties of light for this case ($g_{S_1} \neq 0$, $g_{A_1} \neq 0$, $\xi_{S_1} \neq 0$, $\xi_{A_1} \neq 0$, $n_{V_1} \neq 0$). Fig. 7a shows the photon number distribution $p(n, z)$ for mode (S_1, A_1) , which developed from Poissonian statistics through sub-Poissonian statistics to super-Poissonian statistics and this evolution repeats with increasing z . The corresponding moments of intensity, demonstrating photon antibunching at the corresponding z , are given in Fig. 7b. Squeezing of vacuum fluctuations in mode (S_1, V_1) can be seen in Fig. 8. Increasing values of n_{V_1} smooth out negative moments of intensity. Thus, negative moments in mode (S_1, V_1) cannot occur owing to chaotic phonon statistics (in the opposite to Brillouin scattering) and moments can evolve periodically and they can reach the initial values for longer z . But negative moments of intensity in mode (S_1, V_1) can be induced by linear Stokes coupling ($\kappa_S \neq 0$, $\xi_{S_2} \neq 0$). Non-zero Stokes coupling provides negative moments and squeezing in compound modes composed of single modes in different waveguides, especially in (S_2, A_1) and (S_2, V_1) . No antibunching and squeezing are possible in modes (S_1, S_2) and (V_1, V_2) ($g_{S_2} \neq 0$, $g_{A_2} \neq 0$, $n_{V_2} \neq 0$).

Influence of κ_A on stimulated Stokes and anti-Stokes processes

Similarly as for Brillouin processes, non-zero anti-Stokes coupling ($\kappa_A \neq 0$, $\xi_{A_2} \neq 0$) of waveguide 2 to waveguide 1 with active stimulated Stokes and anti-Stokes processes ($g_{S_1} \neq 0$, $g_{A_1} \neq 0$, $\xi_{S_1} \neq 0$, $\xi_{A_1} \neq 0$, $n_{V_1} \neq 0$) results in gradual degradation of nonclassical properties of light, i.e. the corresponding values of moments of intensity as well as of the parameters characterizing squeezing successively increase. Non-zero anti-Stokes coupling also introduces oscillations to the spatial development of all the quantities under discussion, in agreement with the fact that the anti-Stokes interaction has tendency to conserve the initial photon statistics.

Influence of κ_S on stimulated Stokes and anti-Stokes processes in both waveguides

In this case, nonclassical effects occur in the same compound modes as for Brillouin processes discussed above, i.e. negative moments of intensity and squeezing can occur in compound modes (S_1, A_1) , (S_1, V_1) , (S_2, A_2) , (S_2, V_2) , (S_2, A_1) , (S_2, V_1) , (S_1, A_2) , and (S_1, V_2) .

Moments of intensity in mode (A_1, V_2) cannot be negative, but values of moments for smaller z can be gradually reduced when z increases, as is shown in Fig. 9.

Non-zero values of κ_S introduce oscillations to spatial development of discussed quantities.

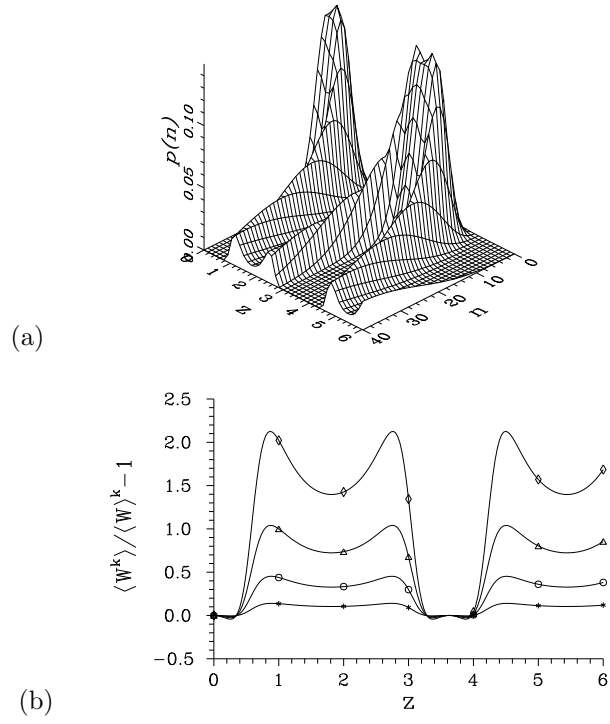


Figure 7: Photon number distribution $p(n, z)$ **(a)** and reduced moments of the integrated intensity $\langle W^k(z) \rangle / \langle W(z) \rangle^k - 1$ for $k = 2$ (*), $k = 3$ (\circ), $k = 4$ (Δ), and $k = 5$ (\diamond) **(b)** for mode (S_1, A_1) ; $g_{S_1} = 1$, $g_{A_1} = 2$, $\xi_{S_1} = -2i$, $\xi_{A_1} = 2i$, $n_{V_1} = 0.1$, and the other parameters are zero.

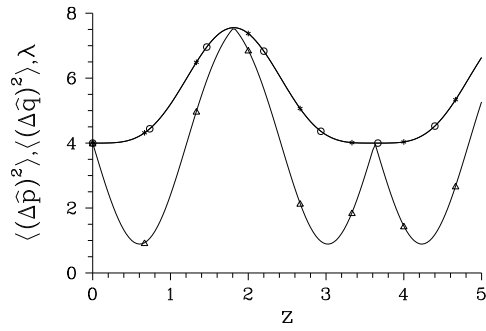


Figure 8: Quadrature variances $\langle (\Delta \hat{p}(z))^2 \rangle$ (*), $\langle (\Delta \hat{q}(z))^2 \rangle$ (\circ), and principal squeeze variance $\lambda(z)$ (Δ) for mode (S_1, V_1) ; $n_{V_1} = 1$ and the other parameters are the same as in Fig. 7.

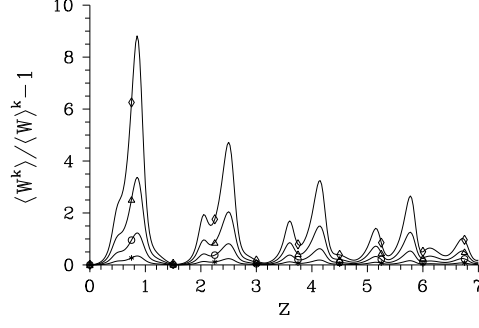


Figure 9: Reduced moments of the integrated intensity $\langle W^k(z) \rangle / \langle W(z) \rangle^k - 1$ for $k = 2$ (*), $k = 3$ (○), $k = 4$ (△), and $k = 5$ (◇) for mode (A_1, V_2) ; $g_{S_1} = 1, g_{A_1} = 2, \kappa_S = -6, g_{S_2} = 1, g_{A_2} = 2, \xi_{S_1} = -2i, \xi_{A_1} = 2i, n_{V_1} = 0.1, \xi_{S_2} = 2, n_{V_2} = 0.1$, and the other parameters are zero.

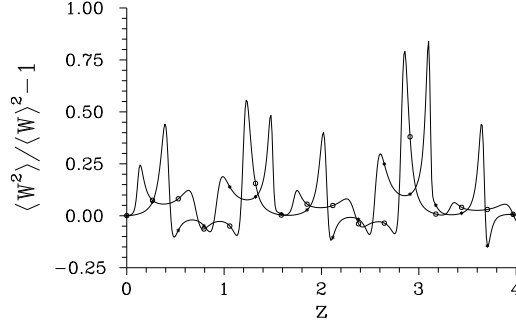


Figure 10: The second reduced moments $\langle W^2(z) \rangle / \langle W(z) \rangle^2 - 1$ for modes (S_1, V_2) (*) and (S_2, V_1) (○); $g_{S_1} = 1, g_{A_1} = 2, \kappa_S = 6i, g_{S_2} = 1, g_{A_2} = 2, \xi_{S_1} = -2i, \xi_{A_1} = 2i, n_{V_1} = 0.1, \xi_{S_2} = -2i, \xi_{A_2} = 2i, n_{V_2} = 0.1$, and the other parameters are zero.

Complex values of κ_S introduce asymmetry into spatial development of the statistical quantities, which affects mainly moments of intensity (see Fig. 10 for moments (S_1, V_2) and (S_2, V_1)). The reduction of initial noise in compound modes can be obtained, including phonon modes V_1 and V_2 .

Influence of Stokes and anti-Stokes couplings on Raman processes in both waveguides

The configuration from the previous section can be extended by including anti-Stokes coupling ($\kappa_A \neq 0$). Negative moments of intensity and squeezing occur in the same compound modes as discussed in the previous section, provided that the values of the anti-Stokes coupling constant κ_A are small. Greater values of κ_A provide greater values of moments of intensity. Fig. 11 shows the spatial development of the second moment of intensity of mode (S_1, A_1) , which is negative only for smaller values of z . Greater values of κ_A lead to a complete loss of negative values of moments for compound modes, in which they can occur for smaller values of κ_A . They also cause a successive increase of values of variances and uncertainty with increasing z in the most of modes, but squeezing for greater z can be also reached in some modes (e.g. $(S_1, A_1), (S_2, A_2)$).

Greater values of n_{V_1} and n_{V_2} preserve negative moments of intensity and squeezing in compound modes excluding phonon modes $((S_1, A_1), (S_2, A_2), (S_2, A_1), (S_1, A_2))$. They destroy non-classical effects in compound modes involving phonon modes V_1 and V_2 .

Negative moments of intensity cannot be obtained in mode (V_1, V_2) , but initial greater values of moments can be substantially reduced.

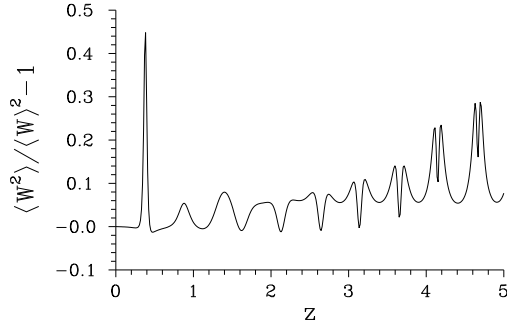


Figure 11: The second reduced moment of the integrated intensity $\langle W^2(z) \rangle / \langle W(z) \rangle^2 - 1$ for mode (S_1, A_1) ; $\kappa_A = 6i$ and the other parameters are the same as in Fig. 10.

If we compare the above results for couplers with Brillouin and Raman processes, we can conclude that in both the cases sub-Poissonian photon statistics and squeezing of vacuum fluctuations can occur in both compound modes of one waveguide $((S_j, A_j), (S_j, V_j), j = 1, 2)$ and compound modes consisting of single modes in different waveguides $((S_1, A_2), (S_1, V_2))$. The Stokes linear coupling supports nonclassical properties of light, whereas the anti-Stokes linear coupling destroys them. Both Stokes and anti-Stokes linear coupling constants introduce oscillations to spatial development of the statistical quantities under discussion.

5 Conclusions

We have investigated nonlinear optical couplers composed of two waveguides operating by means of Brillouin or Raman processes, which mutually interact through linear Stokes and anti-Stokes couplings. We have solved the model, assuming classical strong laser pump modes, analytically for special cases and in short-length approximation as well. General solutions have been obtained numerically. We have investigated the statistical properties of single and compound modes, in particular we have obtained photon number distributions, reduced moments of the integrated intensity, quadrature variances, principal squeeze variance and uncertainty product. It has been shown that nonclassical light can be generated only in the compound modes. Light exhibiting sub-Poissonian photon statistics and squeezing of vacuum fluctuations can be obtained in both compound modes of one waveguide $((S_j, A_j), (S_j, V_j), j = 1, 2)$ and compound modes composed of single modes in different waveguides $((S_1, A_2), (S_1, V_2))$. The linear Stokes coupling supports nonclassical light generation, whereas the linear anti-Stokes coupling leads to its degradation. Both Stokes and anti-Stokes couplings introduce oscillations into spatial development of the statistical quantities. The above conclusions are valid for both Brillouin and Raman processes. However, in Raman processes, increasing values of the mean phonon numbers degrade nonclassical light, especially in compound modes involving phonon modes.

6 Acknowledgments

This work was supported by the Complex Grant VS96028 of Czech Ministry of Education and by the Grant 202/96/0421 of Czech Grant Agency.

References

- [1] Assanto G, Laureti-Palma A, Sibilica C and Bertolotti M 1994 *Optics Commun.* **110** 599
- [2] Peřina J and Bajar J 1995 *J. Mod. Optics* **42** 2337

- [3] Mišta L and Peřina J 1997 Symmetric directional coupler *Czech. J. Phys.* at press
- [4] Peřina J 1995 *J. Mod. Optics* **42** 1517
- [5] Peřina J and Peřina Jr J 1995 *Quant. Semiclass. Optics* **7** 541
- [6] Peřina J and Peřina Jr J 1995 *Quant. Semiclass. Optics* **7** 863
- [7] Peřina J and Peřina Jr J 1995 *Quant. semiclass. Optics* **7** 849
- [8] Peřina J and Peřina Jr J 1996 *J. Mod. Optics* **43** 1951
- [9] Janszky J, Sibilia C, Bertolotti M, Adam P and Petak A 1995 *Quant. Semiclass. Optics* **7** 509
- [10] Mogilevtsev D, Korolkova N and Peřina J 1996 *Quant. Semiclass. Optics* **8** 1169
- [11] Mogilevtsev D, Korolkova N and Peřina J 1997 Band-gap quantum coupler *J. Mod. Optics* at press
- [12] Korolkova N and Peřina J 1997 Quantum statistics of symmetrical optical parametric nonlinear coupler *Opt. Commun.* at press
- [13] Chefles A and Barnett S M 1996 *J. Mod. Optics* **43** 709
- [14] Korolkova N and Peřina J 1996 *Opt. Commun.* **136** 135
- [15] Korolkova N and Peřina J 1997 Kerr nonlinear coupler with varying linear coupling coefficient *J. Mod. Optics* submitted
- [16] Raymer M G and Walmsley I A 1990 *Progress in Optics* Vol. 28 ed. E Wolf (Amsterdam: North-Holland) p. 181
- [17] Miranowicz A and Kielich S 1993 *Modern Nonlinear Optics* Vol. 3 eds. M W Evans and S Kielich (New York: J Wiley) p. 531
- [18] Peřina J 1991 *Quantum Statistical Properties of Linear and Nonlinear Optical Phenomena* 2nd edn (Dordrecht: Kluwer)
- [19] Pieczonková A and Peřina J 1981 *Czech. J. Phys.* **B 31** 837
- [20] Pieczonková A 1982 *Czech. J. Phys.* **B 32** 831
- [21] Peřina J, Kárská M and Křepelka J 1991 *Acta Phys. Pol.* **A 79** 817
- [22] Chizhov A V, Haus J W and Yeong K C 1995, *Phys. Rev. A* **52** 1698
- [23] Yeong K C, Haus J W and Chizhov A V 1996 *Phys. Rev. A* **53** 3606
- [24] Vodchitz A I, Kozich V P, Apanasevich P A and Orlovich V A 1996 *Opt. Commun.* **125** 243
- [25] Werner M J 1996 *Phys. Rev. A* **54** R2567
- [26] Gerdjikov V S and Kostov N A 1996 *Phys. Rev. A* **54** 4339
- [27] Peřina J and Křepelka J 1991 *J. Mod. Optics* **38** 2137
- [28] Peřina Jr J 1993 *J. Mod. Optics* **40** 2105